

Electron Spin Resonance

David J. Lurie, PhD

Bio-Medical Physics, School of Medical Sciences,
University of Aberdeen, Foresterhill, Aberdeen, AB25 2ZD, UK

1. Introduction

The vast majority of magnetic resonance imaging and spectroscopic investigations make use of nuclear magnetic resonance (NMR), exploiting the interactions of atomic nuclei with applied static and radiofrequency magnetic fields. Nevertheless, there exists another important “flavour” of magnetic resonance, called Electron Spin Resonance (ESR) – or, interchangeably, Electron Paramagnetic Resonance (EPR) – which can also provide extremely useful information in bio-medical applications. As its name suggests, ESR relies on interactions with electron spins, specifically *unpaired* electron spins, usually located in free radical molecules. Like NMR, ESR can be used in both spectroscopic and imaging modes. Several reviews of this topic have been published [1-6]. The recent volume edited by Berliner contains many review articles pertinent to bio-medical ESR [7].

2. ESR Basics

The fundamental physics of ESR is, in fact, identical to that of NMR. An unpaired electron has a quantum-mechanical spin of $\frac{1}{2}$ so, like the proton in ^1H NMR, can occupy one of two possible orientations relative to an applied magnetic field. These correspond to a low-energy state, with the electron spin aligned parallel to the applied magnetic field \mathbf{B}_0 , and a high-energy state in which the electron spin is aligned against the applied magnetic field. The energy difference between these states, ΔE , is given by

$$\Delta E = g \beta B_0 \quad (1)$$

where g is termed the “ g -factor” and is approximately 2. β is a physical constant known as the Bohr magneton. Resonance occurs when electromagnetic radiation with photon energy equal to ΔE is applied to the sample; the frequency, ν_0 , of this radiation can be predicted through the “Bohr relationship” $\Delta E = h \nu_0$, where h is Planck’s constant. Therefore the frequency is given by

$$\nu_0 = \Delta E/h = g \beta B_0 / h \quad (2)$$

or

$$B_0 = \nu_0 h / g \beta \quad (3)$$

Equation (2) is exactly analogous to the well-known equation $\nu_0 = (\gamma/2\pi)B_0$ from NMR. In the case of ESR the gyromagnetic ratio in frequency units ($\gamma/2\pi$) is replaced by $g \beta / h$, the value of which is equivalent to 659 times the proton gyromagnetic ratio, i.e. 28 GHz/T.

In a manner exactly analogous to the basic NMR experiment, the basic concept of ESR is to apply electromagnetic radiation at the correct frequency to promote electron spins from the low to the high energy state, then to detect the radiation emitted when electrons return to the low energy state.

3. Differences between NMR and ESR

3.1 Resonant Frequency

One important difference between NMR and ESR is that in ESR the resonant frequencies tend to be much higher, by virtue of the 659-times higher gyromagnetic ratio of an unpaired electron relative to a proton. For example, a typical magnetic field strength used in ESR spectrometers is 0.35 T, with a corresponding resonant frequency of about 9.8 GHz. This frequency range is known as “X-band”, and the spectrometer as an “X-band ESR spectrometer”. Such spectrometers are readily available “off the shelf” from a (small) number of commercial sources.

X-band ESR spectrometers are typically used to study small solid samples, or non-aqueous solutions up to a few hundred μL in volume. They cannot be used for biological samples, or for *in vivo* studies, because of the strong non-resonant absorption of microwaves at 9.8 GHz. For that reason, ESR spectrometers (and imagers) have been constructed to operate at lower magnetic fields, and correspondingly lower frequencies, including at “L-band” (about 40 mT and 1 GHz) to study mice and “radiofrequency” (about 10 mT and 300 MHz) to study rats.

3.2 Relaxation Times

The second important difference between NMR and ESR is the typical relaxation times encountered. In bio-medical proton NMR the relaxation times T_1 and T_2 are typically of the order of 0.1 to 1 sec. In bio-medical ESR the equivalent *electron* relaxation times are a million times shorter, i.e. 0.1 to 1 μsec ! The extremely short relaxation times have important implications on the way in which ESR measurements are carried out.

4. Detection of ESR Signals

4.1 Pulsed (Time-Domain) ESR

It is possible to carry out ESR experiments in the same way as NMR is normally done – i.e. by applying a pulse of electromagnetic radiation at the resonant frequency, in a fixed magnetic field, then detecting the transient response of the electron spins, in the form of a free induction decay (FID) signal; electron spin echo measurements can also be performed by including 180° refocusing pulses, again as in NMR. In order to obtain ESR spectroscopic information, the FID or echo signal would be sampled in the time domain, then Fourier transformed.

The difficulty of pulsed ESR, particularly in bio-medical applications, is that the electron relaxation times are so short. In NMR the experimenter has the luxury of 10s of milliseconds to apply the excitation and sample the signal; in ESR the whole excitation and signal sampling procedure must be carried out in a few microseconds at most! The hardware necessary to do this is considerably more sophisticated than that used in NMR.

In practice, pulsed ESR is really only suitable for experiments involving “contrast agents” with relatively long relaxation times ($\sim 1 \mu\text{s}$), such as the oxygenation-sensitive “TAM” radicals developed by Nycomed Innovation (now part GE Healthcare) in Sweden [8]. The ESR spectroscopy/imaging research group at NCI (Bethesda) has developed and used time-domain ESR, mainly directed at tumour oxygenation applications [9-11].

4.2 Continuous-wave ESR

The majority of bio-medical ESR studies make use of free radicals with relaxation times that are too short (i.e. $\ll 1 \mu\text{s}$) to be detected by time-domain ESR. In this case it is necessary to use a radically different method of signal detection, namely continuous-wave (CW) ESR. (Note that, prior to the introduction of FT NMR in the 1970s, many NMR measurements also used CW detection.) CW ESR involves the following steps:

- The sample is placed in a resonator (called a “cavity” at X-band), tuned to the fundamental resonant frequency ν_0 , based on the field strength in use (see equation (2)). The resonator is the equivalent of the RF coil used in NMR. With the sample in place, the resonator is matched to the characteristic impedance of the system, typically 50Ω .
- The resonator is driven with a *continuously-applied*, low-power signal at frequency ν_0 .
- In order to detect the ESR resonance(s), the magnetic field B_0 is swept slowly in amplitude, starting below resonance and ending above resonance. A typical field sweep might cover a range of 10 mT, taking 10 seconds to complete.
- When resonance is reached, the electron magnetization will be affected, altering the sample’s susceptibility. The resulting change in impedance of the resonator (by a small amount) causes some of the applied signal to be reflected from the resonator, and this reflected signal is detected – it is essentially the ESR signal.
- The ESR absorption spectrum is recorded as a graph of reflected signal *versus* applied magnetic field strength.

4.2.1 Magnetic field modulation

In practical implementations of CW-ESR, a method called magnetic field modulation is always used in order to boost the signal-to-noise ratio (SNR). This is necessary because the change in the reflected signal when the magnetic resonance condition is satisfied is actually very small, barely above the noise level. Briefly, this involves superimposing an oscillating magnetic field on the swept magnetic field. The oscillating field is in the same direction as the swept field, but has a much lower amplitude (between $10 \mu\text{T}$ and $100 \mu\text{T}$, compared with the swept field’s 0.35 T or so at X-band). The modulation frequency is usually about 100 kHz.

During the magnetic field sweep, as resonance is approached, the electron spins will come into and out of resonance at the modulation frequency, causing the amplitude of the reflected signal to be modulated at this same frequency. The trick that allows a huge improvement in the SNR of the ESR spectra is *only* to recognise as a

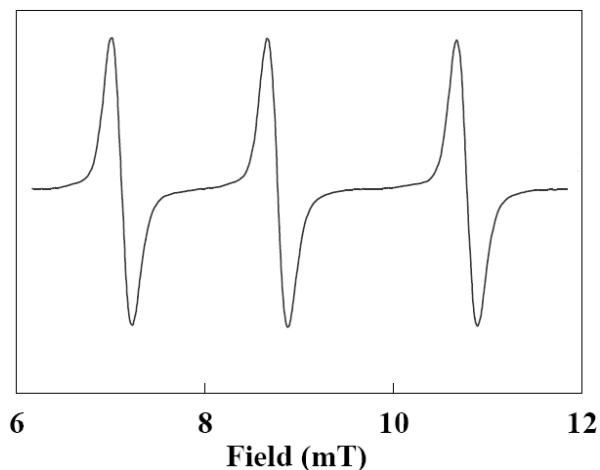


Figure 1: 260 MHz CW-ESR spectrum of 280 ml 2 mM aqueous solution of TEMPOL free radical. The triplet spectrum is characteristic of nitroxide free radicals such as TEMPOL, in which the unpaired electron is located on a nitrogen-oxygen bond. The proximity of the ^{14}N nucleus (spin 1) results in “hyperfine splitting” of the unpaired electron’s ESR resonance, the three lines corresponding to the different allowed orientations of the ^{14}N nucleus in the applied magnetic field.

true signal variations in the signal which occur *at the modulation frequency*. Most sources of noise will not occur at this frequency, so will be rejected. The vital item of hardware in the CW-ESR spectrometer which accomplishes this is called a “lock-in amplifier”.

Because of the way in which lock-in detection is implemented, EPR spectra are virtually always displayed as first derivative spectra – i.e. the *slope* of the absorption spectrum is plotted as a function of magnetic field strength, as opposed to the absorption spectrum itself. Figure 1 shows a typical ESR spectrum obtained from a solution of the stable free radical TEMPOL.

5. ESR Imaging (ESRI)

The above has described how ESR spectra can be produced. In many studies spectra alone are sufficient to obtain valuable chemical and/or physical information about the sample. In other cases, however, it can be extremely useful to be able to generate images showing the spatial distribution of a free radical contrast agent throughout the volume of the sample – hence there is a need for ESR-based imaging. A brief description of ESR imaging (ESRI) will be presented here, and the reader is directed to the following references for more detailed information [1, 2].

5.1 Differences between ESR and NMR imaging

ESRI is very closely related to NMR-based MRI, the two major differences between the techniques being the type of magnetic resonance used (i.e. ESR vs. NMR) and the method of signal detection (i.e. CW-ESR vs. pulsed NMR). However, the idea at the heart of ESRI is exactly the same as the basic component of MRI, namely the use of a magnetic field gradient to “encode” spatial information about the sample into the magnetic resonance signals.

5.2 Projection-reconstruction CW-ESR imaging

In contrast to the pulsed magnetic field gradients used in MRI, however, in CW-ESRI the magnetic field gradients must be applied for the duration of each sweep of the magnetic field through resonance. In other words, the usual sweep of the magnetic field is performed *while the magnetic field gradient is applied* across the sample. Considering a gradient applied in the x-direction, for example, while the magnetic field gradient G_x is switched on, parts of the sample located at positions designated by larger values of x will always experience a higher magnetic

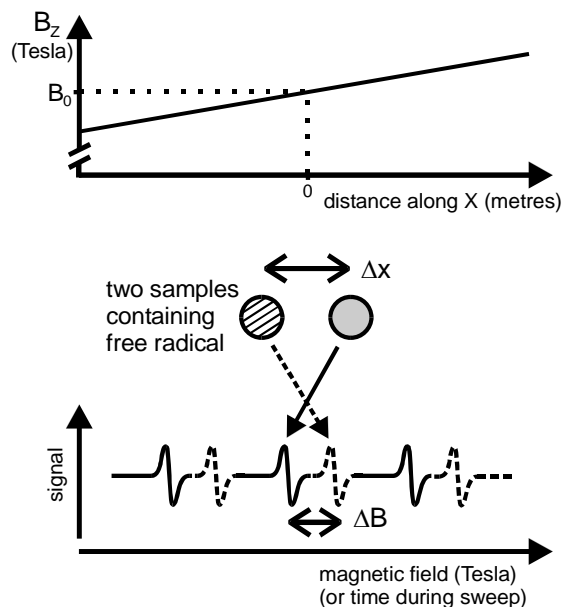


Figure 2: If a continuous magnetic field gradient is applied in the X-direction, the right-hand sample is always at a higher magnetic field than the left-hand sample. Therefore, when the magnetic field is swept the right-hand sample reaches resonance before the sample on the left, and each peak of the nitroxide triplet is split. The solid-line peaks arise from the right-hand sample and the dashed-line peaks from the sample on the left. If the distance between the centres of the samples is Δx , and the gradient strength is G_x , the splitting ΔB is given by $\Delta B = G_x \Delta x$.

field than those located at smaller x values. When the magnetic field sweep is made, unpaired electrons located at large x values will come into resonance earlier than those at smaller x positions. This is demonstrated in Figure 2, which shows the effect on the ESR spectrum of applying a field gradient across a sample consisting of two free radical-containing tubes. The usual 3-line EPR spectrum is split into two, the separation ΔB being directly proportional to the spatial separation Δx of the tubes along the gradient direction.

In general, an object under study will have a continuous variation of concentration of free radical, rather than being confined to two well-defined tubes. In this case, the integral of the EPR spectrum recorded in the presence of a magnetic field gradient represents a one-dimensional projection of the spin-density of the object along the direction of the applied magnetic field gradient. In order to generate data from which a two-dimensional image can be formed, a number of such projections at a range of angles through the sample are obtained, by sequentially applying magnetic field sweeps with the magnetic field gradient applied each time at a different angle with respect to the sample. Following data collection, the image can be reconstructed using filtered back-projection. This procedure can easily be extended to obtain three-dimensional images of the distribution of paramagnetic species in a sample, by applying the magnetic field gradient at an appropriate range of angles in three dimensions.

5.3 Problems with ESR imaging

“Pure” ESR imaging, as described above, is capable of imaging the distribution of many free radical contrast agents *in vitro* and *in vivo*. However, it does suffer from some problems:

- (a) ESR linewidths tend to be large (another way of saying that ESR relaxation times are short), resulting in relatively poor spatial resolution in many cases – images can appear blurred in comparison with proton MRI.
- (b) Slice-selective excitation is not possible in CW-ESR imaging, so 2-dimensional imaging with well-defined slices cannot be done. Imaging tends to be 3D, which either takes a long time, or else sacrifices spatial resolution.
- (c) ESR images show only the location of free radicals, so the anatomy cannot be visualised.

6. Overhauser Effect-based Imaging

Free radical imaging methods based on the Overhauser effect have been developed to address the above problems. The resulting technique is known as Proton-Electron Double-Resonance Imaging (PEDRI) [3, 12] or as Overhauser MRI (OMRI) [13]; henceforth the former acronym will be used here.

6.1 The Overhauser effect

The Overhauser effect, also known as “dynamic nuclear polarisation” (DNP), was predicted by Overhauser in 1953 [14]. In any sample containing paramagnetic molecules in solution (such as a biological sample or animal containing free radicals) interactions will occur between the unpaired electrons and the NMR-sensitive hydrogen nuclei (protons) in the solvent water molecules. In the Overhauser effect an NMR experiment is carried out to detect an NMR signal from the water protons, and at the same time the sample is irradiated at the ESR frequency to excite the unpaired electron spins. The result of the ESR irradiation can be a significant

enhancement (or amplification) of the measured NMR signal, relative to the signal obtained without ESR irradiation.

6.2 PEDRI

In PEDRI the sample under study is irradiated at the ESR frequency of the free radical under study, during the collection of an MR image. NMR signals from regions of the sample containing the free radical are enhanced by the Overhauser effect, and will exhibit correspondingly increased intensity in the MR image, revealing the distribution of the free radical. As is the case with ESR spectroscopy and imaging of biological samples (see section 3.1

above), PEDRI must be implemented at sufficiently low magnetic field (i.e. low enough ESR frequency) that the ESR irradiation is (a) able to penetrate into the sample and (b) does not overheat the sample through non-resonant absorption. To date, *in vivo* PEDRI studies have been performed on mice at a magnetic field of 20 mT, with EPR irradiation at 560 MHz [15], and on rats at 10 mT, with EPR irradiation at 237 MHz [13, 16]. Figure 3 shows a typical PEDRI pulse sequence. Frequently PEDRI is applied in an interleaved fashion, ESR-on and ESR-off, to allow simultaneous collection of Overhauser-enhanced and unenhanced images; subtraction of the data sets then produces an image showing only the distribution of free radicals.

6.3 Field-cycled PEDRI (FC-PEDRI)

Despite the use of low magnetic field strengths, excessive non-resonant power deposition in biological samples may still be problematic in PEDRI experiments, because the Overhauser enhancement is maximised by near-saturation of the ESR. Even lower field strengths than 10 mT could be used, in order to reduce the ESR irradiation frequency and hence lower the absorbed power. However, the use of very low field strengths will also result in a reduction of the SNR of the NMR experiment, leading to poor image quality (despite the Overhauser enhancement). Field-Cycled PEDRI (FC-PEDRI) was developed to counter this problem [3, 17].

In FC-PEDRI the magnetic field strength, B_0 , is switched between two values during the pulse sequence, as shown in Figure 4. The field is reduced to B_0^E (~ 5 mT) for the evolution period, during which the ESR irradiation is applied. Since B_0^E is low, the ESR frequency and power deposition are also low. During this period the Overhauser enhancement of the proton magnetisation occurs. The field is then ramped up to the detection value, B_0^D , and the NMR RF pulse(s) and imaging gradients are applied. Because B_0^D is higher, the SNR of the imaging experiment is increased.

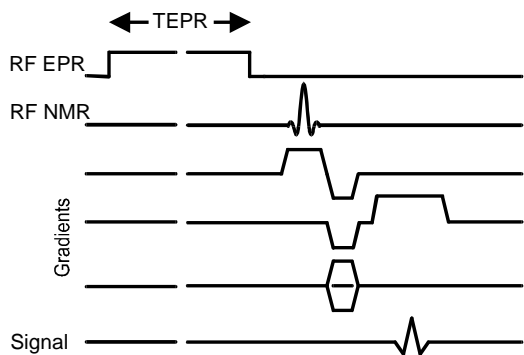


Figure 3: Typical PEDRI pulse sequence. ESR irradiation (shown as RF EPR) lasts for a time $TEPR$, which should ideally be at least 3 times the NMR T_1 .

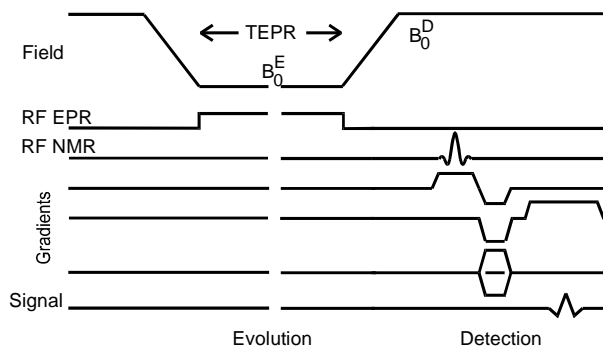


Figure 4: Typical Field-cycled PEDRI pulse sequence.

We have constructed an FC-PEDRI imager with a large field-cycling magnet [18]. This instrument uses a double magnet system. A human whole-body sized ferrite permanent magnet provides the vertically-oriented detection field (B_0^D) of 59 mT. Inside the bore of the permanent magnet is mounted a resistive magnet coil which can partially cancel the field from the permanent magnet. With this system the magnetic field can be ramped from 5 mT to 59 mT in 40 ms. Another system has been constructed in our lab for imaging free radicals in small animals; in this system the primary magnet is a 0.45 T superconducting magnet, while the field-cancellation coil is a resistive, actively-shielded solenoid [19].

7. Applications of ESR

The main purpose of this paper has been to compare the physical and technological aspects of ESR and NMR, as used in a bio-medical context. To conclude, some applications of ESR will be mentioned briefly.

The majority of applications of ESR to date have involved the use of stable free radical “probes”, such as the previously-mentioned TAM [8] or nitroxide free radicals [20]. As well as these soluble probes, solid probes also play a role, in single crystal or particulate forms, especially in the measurement of oxygen concentration [21].

ESR is able to obtain useful information by virtue of the dependence of the ESR spectral characteristics (linewidth and/or line splitting) on physical and chemical parameters. This is the basis of “ESR oximetry” [22] (which has begun to be used clinically [23]) and of pH measurement by ESR, using pH-sensitive nitroxides [24].

More challenging is the detection of naturally-occurring free radicals, such as oxygen-derived radicals and nitric oxide; despite difficulties associated with low concentrations and short lifetimes of these molecules, they can be detected with the aid of chemical stabilisation methods called spin-trapping [25].

Most bio-medical applications of ESR to date have been *in vitro*, or *in vivo* in small-animal models, though at least one research group has begun to use ESR spectroscopy in a clinical context, for oximetric measurements [26].

8. References

- [1] G.R. Eaton, S.S. Eaton and K. Ohno eds., *EPR Imaging and In Vivo EPR*, Boca Raton: CRC Press (1991).
- [2] K. Kuppusamy, M. Chzhan and J.L. Zweier, “Principles of Imaging: Theory and Instrumentation,” in *In Vivo EPR (ESR): Theory and Applications*, vol. 18, L.J. Berliner Ed. New York: Kluwer Academic / Plenum Publishers, pp. 99-152 (2003).
- [3] D.J. Lurie, “Proton-Electron Double-Resonance Imaging (PEDRI),” in *In Vivo EPR (ESR): Theory and Applications*, vol. 18, L.J. Berliner Ed. New York: Kluwer Academic / Plenum Publishers, pp. 547-578 (2003).
- [4] D.J. Lurie, “Techniques and Applications of EPR Imaging,” in *Specialist Periodical Reports: Electron Paramagnetic Resonance*, vol. 18, B.C. Gilbert, M.J. Davies and D.M. Murphy Eds. Cambridge: Royal Society of Chemistry, pp. 137-160 (2002).
- [5] D.J. Lurie and K. Mader, “Monitoring drug delivery processes by EPR and related techniques - principles and applications”, *Adv. Drug Deliv. Rev.*, **57**, 1171-1190 (2005).
- [6] H.M. Swartz, N. Khan, J. Buckley, R. Comi, L. Gould, O. Grinberg, A. Hartford, H. Hopf, H.G. Hou, E. Hug, A. Iwasaki, P. Lesniewski, I. Salikhov and T. Walczak, “Clinical applications of EPR: overview and perspectives”, *NMR Biomed.*, **17**, 335-351 (2004).

- [7] L.J. Berliner ed., *In Vivo EPR (ESR): Theory and Applications*, New York: Kluwer Academic / Plenum Publishers (2003).
- [8] J.H. ArdenkjaerLarsen, I. Laursen, I. Leunbach, G. Ehnholm, L.G. Wistrand, J.S. Petersson and K. Golman, "Epr and dnp properties of certain novel single electron contrast agents intended for oximetric imaging [full text delivery]", *J.Magn.Reson.*, **133**, 1-12 (1998).
- [9] M. Afeworki, G.M. van Dam, N. Devasahayam, R. Murugesan, J. Cook, D. Coffin, J.H.A. A-Larsen, J.B. Mitchell, S. Subramanian and M.C. Krishna, "Three-dimensional whole body imaging of spin probes in mice by time-domain radiofrequency electron paramagnetic resonance", *Magn.Reson.Med.*, **43**, 375-382 (2000).
- [10] S. Subramanian, K. Yamada, A. Irie, R. Murugesan, J.A. Cook, N. Devasahayam, G.M. Van Dam, J.B. Mitchell and M.C. Krishna, "Noninvasive in vivo oximetric imaging by radiofrequency FT EPR", *Magn.Reson.Med.*, **47**, 1001-1008 (2002).
- [11] S. Subramanian, K.I. Matsumoto, J.B. Mitchell and M.C. Krishna, "Radio frequency continuous-wave and time-domain EPR imaging and Overhauser-enhanced magnetic resonance imaging of small animals: instrumental developments and comparison of relative merits for functional imaging", *NMR Biomed.*, **17**, 263-294 (2004).
- [12] D.J. Lurie, D.M. Bussell, L.H. Bell and J.R. Mallard, "Proton-Electron Double Magnetic Resonance Imaging of Free Radical Solutions", *J.Magn.Reson.*, **76**, 366-370 (1988).
- [13] K. Golman, I. Leunbach, J.H. ArdenkjaerLarsen, G.J. Ehnholm, L.G. Wistrand, J.S. Petersson, A. Jarvi and S. Vahasalo, "Overhauser-enhanced mr imaging (omri)", *Acta Radiol.*, **39**, 10-17 (1998).
- [14] A.W. Overhauser, "Polarization of nuclei in metals", *Phys. Rev.*, **92**, 411-415 (1953).
- [15] H.H. Li, Y.M. Deng, G.L. He, P. Kuppusamy, D.J. Lurie and J.L. Zweier, "Proton electron double resonance imaging of the in vivo distribution and clearance of a triaryl methyl radical in mice", *Magn.Reson.Med.*, **48**, 530-534 (2002).
- [16] I. Seimenis, M.A. Foster, D.J. Lurie, J.M.S. Hutchison, P.H. Whiting and S. Payne, "The excretion mechanism of the spin label proxyl carboxylic acid (PCA) from the rat monitored by X-band ESR and PEDRI", *Magn.Reson.Med.*, **37**, 552-558 (1997).
- [17] D.J. Lurie, J.M.S. Hutchison, L.H. Bell, I. Nicholson, D.M. Bussell and J.R. Mallard, "Field-Cycled Proton Electron Double-Resonance Imaging of Free Radicals in Large Aqueous Samples", *J.Magn.Reson.*, **84**, 431-437 (1989).
- [18] D.J. Lurie, M.A. Foster, D. Yeung and J.M.S. Hutchison, "Design, construction and use of a large-sample field-cycled PEDRI imager", *Phys.Med.Biol.*, **43**, 1877-1886 (1998).
- [19] D.J. Lurie, G.R. Davies, M.A. Foster and J.M.S. Hutchison, "Field-cycled PEDRI imaging of free radicals with detection at 450 mT", *Magn.Reson.Imaging*, **23**, 175-181 (2005).
- [20] G.L. He, A. Samouilov, P. Kuppusamy and J.L. Zweier, "In vivo imaging of free radicals: Applications from mouse to man", *Mol.Cell.Biochem.*, **234**, 359-367 (2002).
- [21] J.F. Dunn and H.M. Swartz, "In vivo electron paramagnetic resonance oximetry with particulate materials", *Methods*, **30**, 159-166 (2003).
- [22] H.M. Swartz and J.F. Dunn, "Measurements of oxygen in tissues: Overview and perspectives on methods", *Oxygen Transport to Tissue Xxiv*, **530**, 1-12 (2003).
- [23] N. Khan, H.G. Hou, P. Hein, R.J. Comi, J.C. Buckey, O. Grinberg, I. Salikhov, S.Y. Lu, H. Wallach and H.M. Swartz, "Black magic and EPR oximetry: From lab to initial clinical trials", *Oxygen Transport to Tissue Xxvi*, **566**, 119-125 (2005).
- [24] V.V. Khrantsov, I.A. Grigor'ev, M.A. Foster and D.J. Lurie, "In vitro and in vivo measurement of pH and thiols by EPR-based techniques", *Antioxidants & Redox Signaling*, **6**, 667-676 (2004).
- [25] L.J. Berliner, V. Khrantsov, H. Fujii and T.L. Clanton, "Unique in vivo applications of spin traps", *Free Radical Biology and Medicine*, **30**, 489-499 (2001).
- [26] I. Salikhov, T. Walczak, P. Lesniewski, N. Khan, A. Iwasaki, R. Comi, J. Buckey and H.M. Swartz, "EPR spectrometer for clinical applications", *Magn.Reson.Med.*, **54**, 1317-1320 (2005).